

Chapter 4: Steering and Orbit Correction

4.1 Motivation

Precise control of centroid orbit is necessary for good beam recirculation, with low losses due to large centroid deviations. This allows for observation of beam losses due to more complex effects, such as resonant excitation of particle and/or beam envelope amplitudes, as well as longitudinal losses. The proposed quasi-integrable nonlinear optics experiment has, as its lowest-order, most straightforward diagnostic, a characterization of resonantly driven beam losses with and without nonlinear damping. Therefore, a reduction of transverse scraping losses is imperative for observation of these likely slower loss rates. Additionally, the nonlinear optics experiments require a low-current, high-emittance $60\mu A$ beam. A large emittance beam corresponds to a large cross-section beam in configuration space, which places a more stringent requirement on steering tolerances.

In an ideal linear accelerator, there exists a "reference trajectory," which describes the path of an ideal particle. This trajectory is typically centered within the focusing quadrupoles and the beam pipe. A beam with imperfect injection conditions will oscillate about the ideal trajectory. In this section, we define "first-turn orbit" to mean the measured or simulated centroid trajectory on the first

turn. "Closed orbit" refers to the orbit about which the trajectory oscillates. This is also referred to as the "equilibrium orbit." Ideally this orbit is centered in the quadrupoles, but due to background field, alignment errors and number of available correctors, it is only possible to minimize orbit deviation from quadrupole centers.

In general, for straightforward operation of UMER, lowest-possible deviation of beam centroid from quadrupole centers in multi-turn operation is desirable, for the smallest coupling between focusing strength and closed orbit deviation. As seen in Section ??, the dynamic aperture of the quasi-integrable octupole lattice suffers greatly for orbit distortions, and it is desirable to minimize centroid offset from octupole centers in the octupole insert.

4.2 *Considerations for low-rigidity electron beam*

In typical high-energy accelerating or storage rings (for which steering algorithms are well-developed), the beam travels in straight lines between steering elements (dipoles or off-centered quadrupoles), effectively tracing out an N-sided polygon where N is the number of dipoles. Steering in UMER is complicated by the fact that at low-energies, the beam is significantly bent by background, ambient fields. For a 10 keV electron beam, rigidity $B\rho = \frac{p}{q}$ is 338.859 G-cm. The required integrated field to bend the beam 10° is 59.154 G-cm. Given an average ambient vertical field of ≈ 400 mG, per 32 cm cell, the integrated field is $32 * 0.400 = 12.8$ G-cm. Therefore, approximately 22% of the total horizontal bending in the ring is due to the ambient vertical fields. The ambient horizontal field is weaker, on

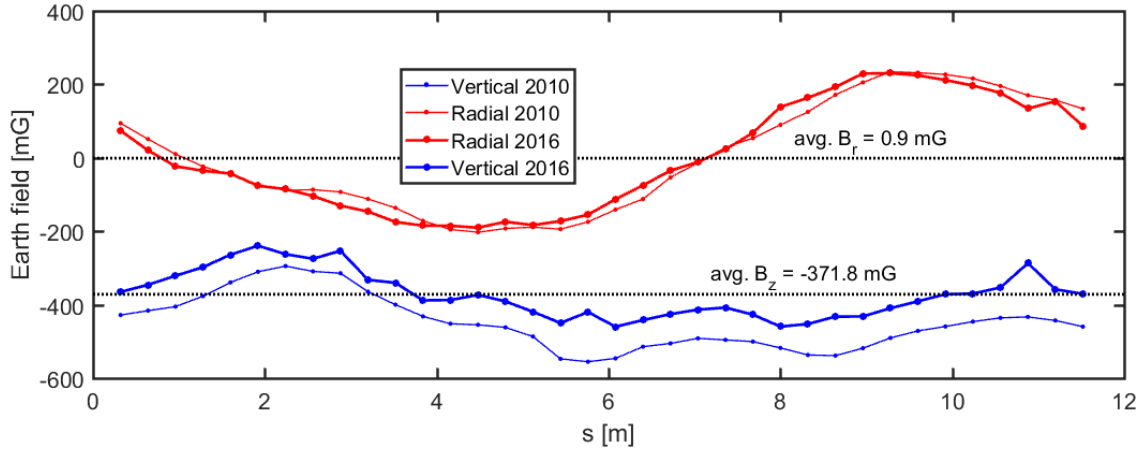


Fig. 4.1: Ambient fields measured at UMER dipoles, from Dave Sutter measurements 6/1/2010 and 7/22/2016.

average < 1 mG, which gives only a small orbit distortion (requiring only a small correction) from turn-to-turn. However, local closed orbit distortions due to the horizontal fields can be large (up to ≈ 200 mG), and large vertical corrections are necessary to minimize deviation from quadrupole centers. Measured ambient field data can be seen in Figs. ?? and ??.

Because the beam is immersed in a bending field, in the perfectly aligned case a beam orbit that is centered in the quadrupoles is required to be displaced in the BPMs, as in Fig. ?. Simple calculations with a constant background field show that we expect the ideal orbit to be radially displaced by [todo:]. However, in the case of azimuthally-varying ambient fields and displacements up to several millimeters, we expect larger displacements of the "best-possible" orbit.

Steering in the ring is controlled by 36 horizontal bending dipoles, which determine the shape of the horizontal closed orbit, and which can be independently

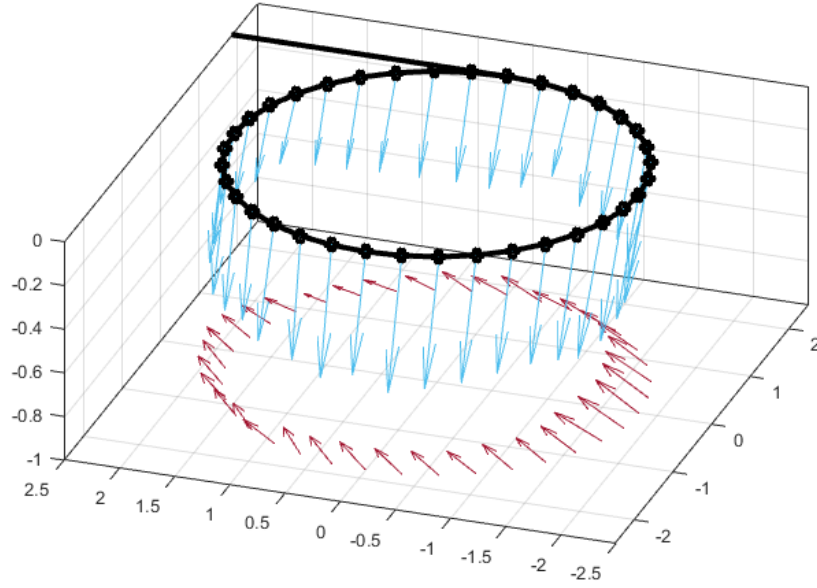


Fig. 4.2: Ambient field data vectors, including xy projection. x,y units are meters, z-axis is milli-Gauss.

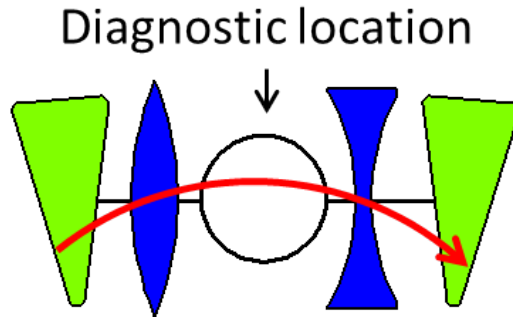


Fig. 4.3: Diagram of beam position in diagnostic (BPM) for an orbit that is horizontally centered in the quadrupoles.

adjusted to optimize the orbit. This is different from the typical case of a larger ring, which uses fixed dipoles and adjustable corrector magnets. There is 1 independent horizontal dipole every 2 quadrupoles. Vertical correction is made with 18 printed circuit corrector magnets located at pipe flanges, which are named "RSV" magnets. There is 1 RSV corrector every 4 quadrupoles. Additional vertical correctors have been added and proposed, as described in Section ???. Steering near injection is controlled by 6 vertical and horizontal corrector magnets in the injection line, in the "SDH" and "SDV" families. Additionally, there are two correctors (one horizontal and one vertical) in the ring near the intersection of the injection pipe (the "Y-section"), named "SDR6H" and "SDR6V."

4.3 *Prior Approach*

An alternative approach to steering was developed using a steering procedure with local corrections to ensure the equilibrium orbit is centered (or as close to centered as possible) in the quadrupoles. This is unique from the response matrix method, in which a global correction is calculated that aims to center the equilibrium orbit at the 14 BPM locations. The steering algorithm is a methodical, "front to back" approach that first minimizes the position of the beam in the quadrupoles on the first turn then minimizes orbit deviations in subsequent turns. This algorithm should result in smaller local orbit excursions from quadrupole centers, since it utilizes 36 position data points at quadrupole locations for the first turn orbit as opposed to 14 at the BPMs. This is proposed as an alternative to the response matrix

steering algorithm [?], and may be more useful for applications where orbit centering in the quadrupoles is essential.

The remainder of this chapter describes the tools and algorithmic approach to centering the first turn orbit in the quadrupole centers. First I describe the quad-as-BPM procedure for measuring first-turn centroid position at the quadrupoles (Section ??). Then I summarize the application of various algorithms to set horizontal and vertical steerers in Section ??, including theoretical "best-case" orbit excursions and proposed vertical steering upgrades to meet the dynamic aperture requirements for the nonlinear optics experiments. This includes first-turn data taken during ring steering tests. Section ?? lays out a sample steering procedure, including injection and multi-turn optimization routines.

4.4 *Quadrupole as BPM technique*

First-turn position data is garnered from quadrupole response data, also called "quad as BPM" or "virtual BPM." A beam that is off-centered in a quadrupole will experience a dipole force acting on the centroid motion as well as a quadrupole focusing force that acts on the beam envelope. The strength of the dipole kick will depend on the position of the centroid in the quadrupole as well as strength of the quadrupole. Variation of the quadrupole strength will cause variation of the centroid as detected on a downstream BPM. Knowledge of the centroid transformation between quadrupole and BPM allows reconstruction of the beam position

The quad as BPM method is a way to measure the beam orbit in the first turn.

We calculate the beam position at the center of each quadrupole by measuring the change in beam position due to a perturbation in the quadrupole current. This is an essentially identical method to that described by Kamal Poor Rezaei in an earlier technical note [?], with the main difference being the use of the VRUMER beam tracking code to calibrate position, rather than a transfer matrix calculation.

In the work described here, calibration of quadrupole response (measured directly at nearest downstream BPM) is accomplished using VRUMER. VRUMER, described in detail in Appendix [TBD], is a simple orbit integrator written in Matlab, originally developed by Irving Haber to model transverse beam centroid behavior and test UMER-specific steering algorithms. The model used here includes the measured background earth field, applied as a continuously acting, lab-frame-position dependent force based on linear interpolation between measurement points at the 36 dipoles. This model does not include centroid kicks as a result of magnet fringe fields or the steering effect of the offset YQ magnet, although the framework can support these refinements.

4.4.1 *Avoiding null points*

Generally, the quad as BPM measurement uses response data from the nearest downstream BPM. However, for certain quad-BPM pairs this may not be appropriate due to the BPM being located near a null point of the betatron oscillation.

There are two reasons why the BPM response will be very flat: the beam is near the center of the quadrupole, or quad-BPM separation is close to $n\frac{\lambda}{2}$ for integer n , where λ is the betatron wavelength. The beam transformation in VRUMER is

not exactly equivalent to the transformation in UMER (VRUMER does not include edge focusing, SC effects, etc). Therefore, quad-BPM separations near $n\frac{\lambda}{2}$, the BPM response slope will be small in both VRUMER and UMER but not identical. (This is true for all quad-BPM pairs, but will generally be a small error).

At an operating point of 1.826 A, the UMER 6 mA beam has $\nu_x = 6.636$, $\nu_y = 6.752$ [?]. This corresponds to betatron wavelengths $\lambda_x = 1.736$ m, $\lambda_y = 1.706$ m. In the VRUMER simulation, horizontal and vertical tunes are equal (no edge focusing), $\nu = 6.293$, equivalently $\lambda = 1.83$ m. This is consistent with the simplifications made in VRUMER.

We can see that the quad-BPM separations for which unusually high x_q , y_q values appear (Table ??) are close to the the VRUMER wavelength $\lambda = 1.83$ m, $\frac{\lambda}{2} = 0.92$ m. There are two inaccuracies that may result from this:

- Quad-BPM separation is close to UMER betatron wavelength (a null in the actual ring). VRUMER sees a small $\frac{\partial x_{BPM}}{\partial I_Q}$ slope and predicts $x_q \sim 0$, while in reality x_q could be fairly large. This is hard to discern from the data, and may artificially obscure bad first-turn steering.
- Quad-BPM separation is close to VRUMER betatron wavelength. If BPM response slope is not very flat (but VRUMER thinks this should be a null point) the VRUMER calculation for x_q blows up. This can be seen in Fig. ??, where QR14, QR32 and QR62 in particular have unphysically large x_q .

In subsequent quad as BPM data in this note, QR14, QR32 and QR62 use the BPM response in the next nearest downstream BPM to avoid artificial blow-up or

Tab. 4.1

Quad #	Nearest BPM	$\Delta S_{Q \rightarrow BPM}$ [m]
QR14	RC5	0.88
QR32	RC11	1.84
QR38	RC11	0.88
QR62	RC17	0.88
QR70	RC1 (turn 2)	0.88

suppression of x_q and y_q . This effect should also be (but is not currently) included in the calculation of errorbars for the quad as BPM data.

4.4.2 Systematic Error in Quad-as-BPM Calibration

The previous section begs the question, what is the amount of systematic error introduced by differences between reality and the model used for calibration (in this case, VRUMER). Most notably, bare tune in the model and measured tune differ by $\Delta\nu_x = 0.340$ horizontally, $\Delta\nu_y = 0.459$ vertically. It is convenient to define phase advance per cell, $\sigma = \frac{2\pi\nu}{36}$. In a lattice with low phase advance per cell (such as UMER, with 66.4° and 67.5° in the x,y planes), the particle motion is approximately sinusoidal, described by:

$$x(s) = A \frac{\sigma}{L} s \quad (4.1)$$

The derivative of this motion is

$$x'(s) = \frac{dX}{ds} = -A \frac{\sigma}{L} \frac{\sigma}{L} s \quad (4.2)$$





4.5 *Ring steering*

4.5.1 *Horizontal Steering Procedure*

Using VRUMER, I explored the effectiveness of various minimization functions on the first-turn beam orbit for a variety of injection conditions and misalignments. The available minimization functions include steering through downstream focusing or defocusing quad (minimize position in a single quad) or minimization of an RMS quantity dependent on position in both downstream quads. In the thin lens approximation for a focusing dipole separated from a defocusing dipole by a drift of distance L , $x'_F = \frac{x_D - x_F}{L}$. I used $x'_F \propto x_D - x_F$ to include x'_F in the RMS minimization term, see Table ??.

Qualitatively, steering by x_D and x_F, x'_F result in almost identical orbits (sub-millimeter differences) that converge very quickly towards the center of the quads given an injection error or quad misalignment. In practice, it is much faster to minimize x_D , as that requires 1 quad scan for every dipole setting rather than 2 quad scans. It also allows interpolation between scanned dipole settings, as the data can be fit to a line and the zero-crossing calculated (the RMS minimization functions do not lend themselves to fitting by a simple function). However, the x_F, x'_F algorithm seems to yield better results in the lab. This may be because of its ability to handle relative misalignments between the focusing and defocusing

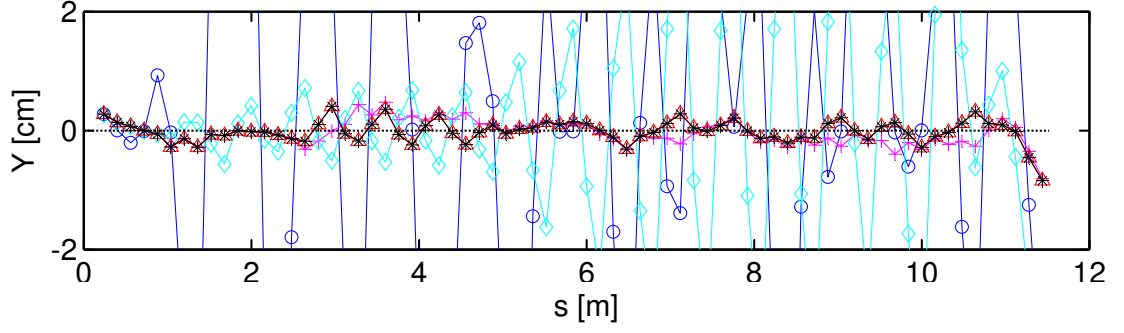
Tab. 4.2: Different algorithms and their performance (RMS position in quads) for initial condition $x = 1\text{mm}$, $x' = 0$.

shorthand	Minimization function	RMS(x_Q) [mm] no misalign.	RMS(x_Q) [mm] $\sigma = 5\text{mm}$	plot trace
x_F	$\ x_F\ $	5.3	37.3	
x_D	$\ x_D\ $	0.2	6.9	
x_F, x_D	$\sqrt{x_F^2 + x_D^2}$	2.1	9.3	
x_F, x'_F	$\sqrt{x_F^2 + (x_D - x_F)^2}$	0.2	6.6	*
x_D, x'_F	$\sqrt{x_D^2 + (x_D - x_F)^2}$	0.2	7.0	

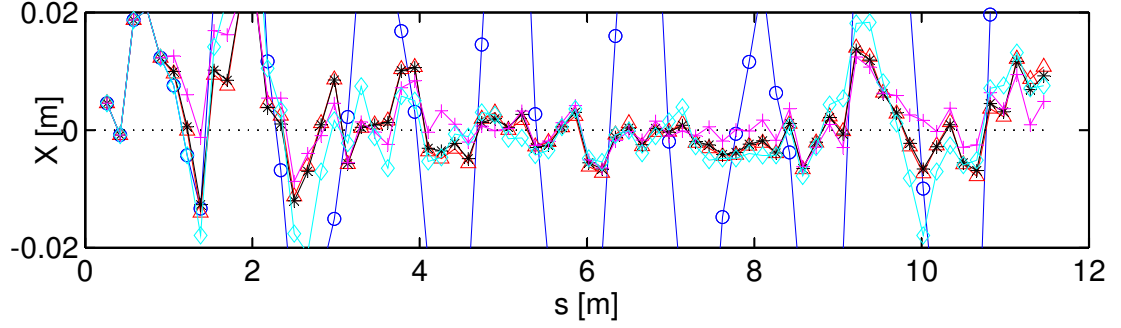
quadrupoles.

The caveats associated with using both of these algorithms will be further discussed in the following section.

A weakness of the $\|x_D\|$ minimization is that occasionally the data will not fall on a straight line. This is most likely due to scraping between the dipole and BPM or noise in the region near the pulser. In the ring steering scripts, I have implemented a points rejection criteria that throws away quad position data with errorbar $> 1\text{ mm}$. As the quad position is proportional to the slope of the beam position in the BPM during the quad scan, the error bar is proportional to the uncertainty in the fitted slope – large nonlinearities in the quad scan data will have large error bars bracketing the estimate of position in the quadrupole. However, some clearly nonlinear points do not have associated large error bars, and one can



(a) No misalignments



(b) Random quad misalignments from Gaussian distribution, $\sigma = 5\text{mm}$

Fig. 4.4: First turn VRUMER orbits for initial condition $x = 1\text{mm}$, $x' = 0$.

still get sidetracked by this effect.

The x_F , x'_F algorithm seems less likely to be led astray by nonlinear response in one of the quads. However, similar problems originating around D15 and D29 arose when using the x_F , x'_F minimization, as seen in Fig. ???. This may be due to misalignments, but will likely be improved by stepping through the ring dipoles for a second steering iteration (at least from D15 onwards).

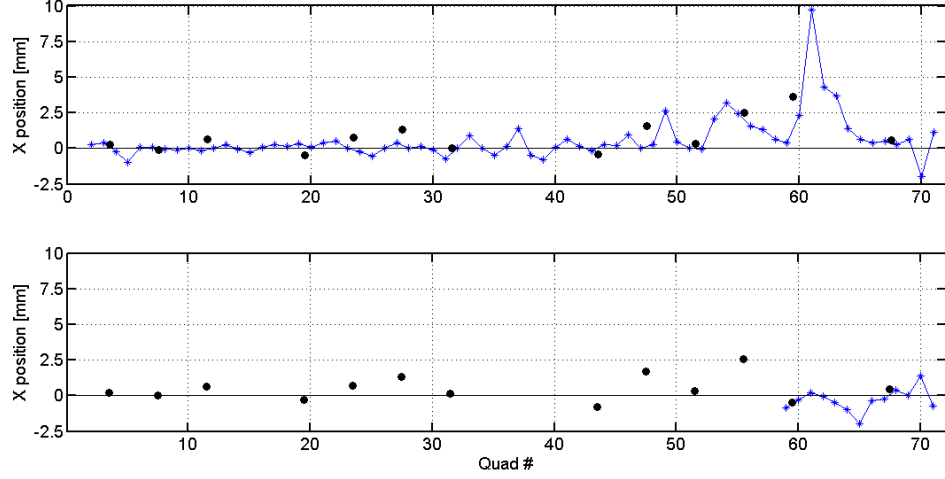


Fig. 4.5: 1st turn solution generated on 11/13/15 (top) and 11/16/15 (bottom), by steering through defocusing quadrupoles.

4.5.2 Vertical Steering Procedure

Vertical steering in UMER is accomplished by 18 vertical correction magnets located at the pipe flanges between plates. All of these magnets are fairly weak, due to the wide bore. With an integrated field of 3.886 G-cm/A, this gives a corrective kick with magnitude $0.66^\circ/\text{A}$. (For comparison, ring dipoles have a correction of $3.4^\circ/\text{A}$.) The largest source of vertical alignment errors is the radial component of the Earth's field, shown in Fig. ???. Although the amplitude 200 mGauss is comparable to the vertical field, the average is only ~ 3 mGauss.

Previous assumption has been that sparsely populated, low-field vertical correctors were sufficient to correct for the low average radial field. Fig. ?? and ?? show measurement of typical vertical steering solution for the 6 mA beam. This solution was obtained by Brian using a trial and error method, settings are saved

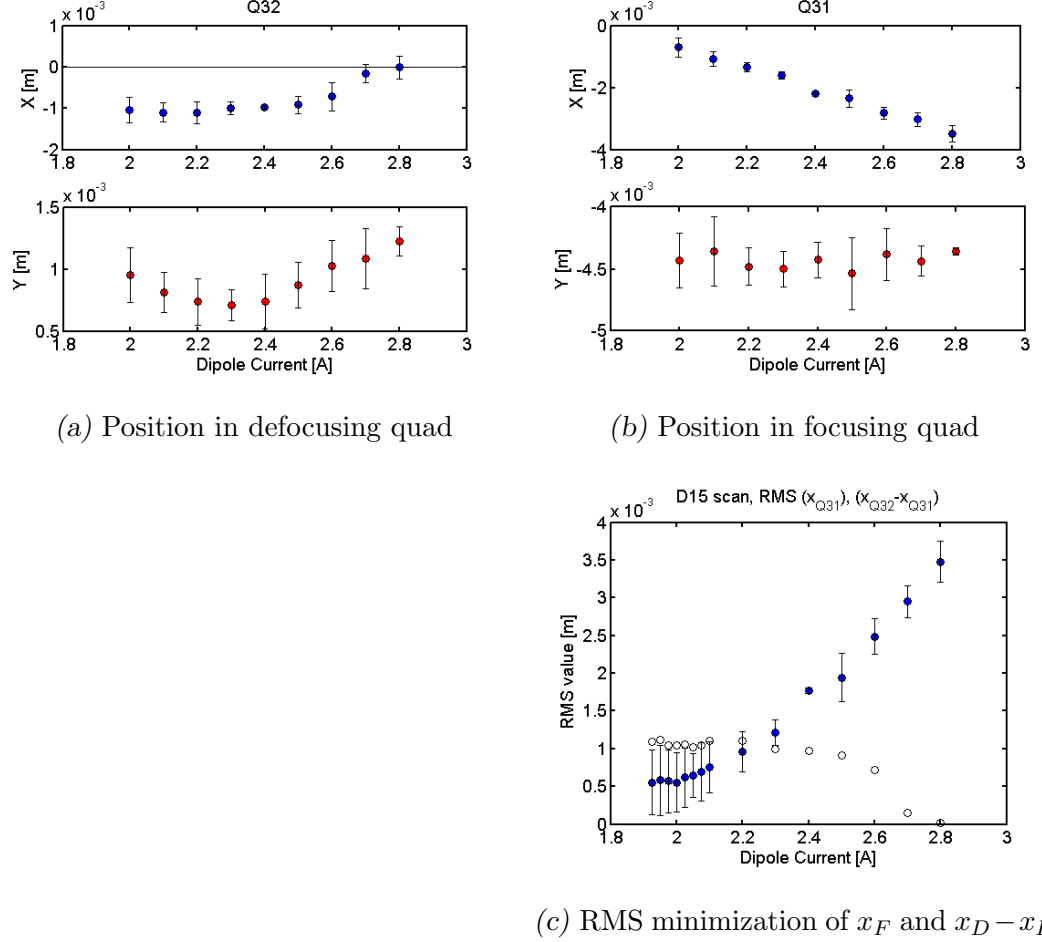
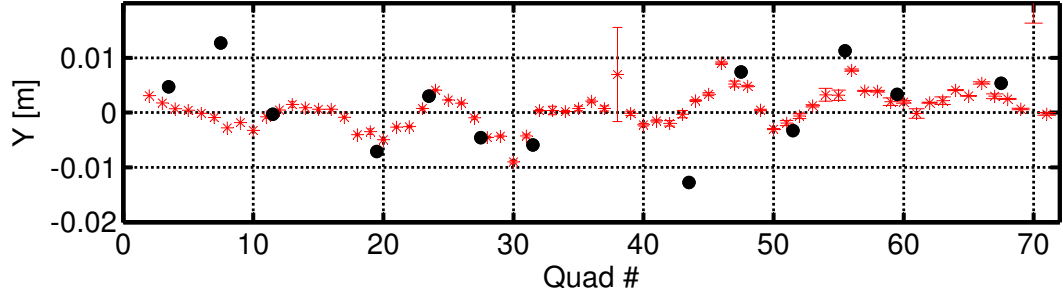


Fig. 4.6: Steering through D15 using two different algorithms, 11/11/15

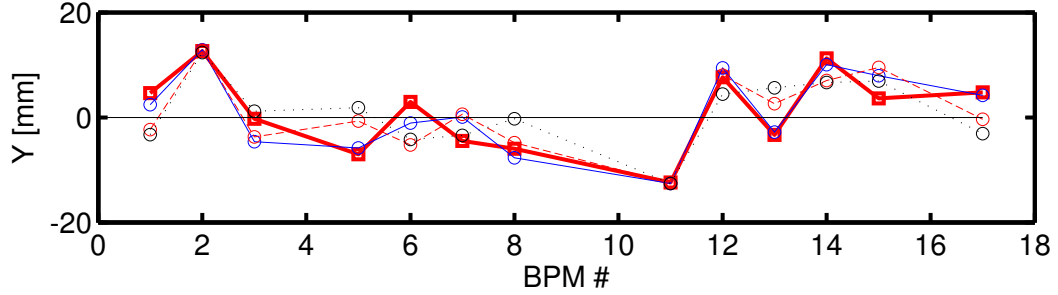
in `kiersten.6mA_151116.csv`. In the first turn, the maximum vertical displacement from quad center is 10 mm and the RMS displacement is 3.2 mm. Deviation about this orbit in the first 4 turns is ~ 10 mm.

This is much worse than the best horizontal steering solution described in this note. For horizontal beam position, the first-turn orbit (Fig. ??) exhibited maximum horizontal displacement of 3.1 mm and RMS displacement of 0.8 mm. Deviation about this orbit in the first 4 turns is ~ 2 mm.

While good recirculation is possible using the existing correctors, an attempt



(a) Vertical position of beam in quads for 1st turn.



(b) Vertical position of beam in BPMs for first 4 turns. Note shorted vertical plates at RC2, RC11.

to steer through the vertical center of the quads will inherently be limited by the strength and density of vertical correctors. We use VRUMER to test various vertical steering algorithms and place a lower bound on the best possible first turn orbit using existing vertical steerers, results are shown in Table ???. This note considers three cases:

- Ideal: Perfect alignment, SV current constrained to be ≤ 10 A.
- SV limit: Perfect alignment, SV current limited to ≤ 2 A.
- Misaligned: Random misalignment, from Gaussian distribution $\sigma = 1$ mm, SV current limited to ≤ 2 A.

In summary, in the ideal case (strong correctors, no mechanical misalignments), we can obtain vertical steering through the quads with comparable accuracy to the measured horizontal solution, $\max(y) \sim 3$ mm, $\text{rms}(y) \sim 1$ mm. This requires maximum SV currents in the range 3-4 A. If we restrict ourselves to 2 A in the SVs, we are now limited to best possible solution $\max(y) \sim 7$ mm, $\text{rms}(y) \sim 2$ mm. Additionally, allowing for random vertical misalignments of order 1 mm, this increases to $\max(y) \sim 10$ mm, $\text{rms}(y) \sim 3 - 4$ mm.

I conclude that the existing vertical correctors provide too weak of a correction to offer significant improvement on the existing first-turn solution (Fig. ??). Also, closing the orbit will likely be more difficult as the adjustability of y, y' at the recirculation point will be limited. Any experiments that require multi-turn operation with modified quadrupole strengths, as well as the nonlinear optics experiments, would benefit from improved control over the vertical orbit. Continued work will investigate the effectiveness of increasing the number of vertical steerers.

4.6 Implementation

The quad as BPM measurement is controlled by UMER control script `kiersten_quad_scan_v2.m`. In this procedure, the current in each ring quadrupole (RQ2-RQ71) is independently scanned about it's nominal operating point. The horizontal and vertical position of the nearest downstream BPM is recorded. This data is fitted to a linear curve, using the linear least squares method. The fitted slope is the BPM response to the quad scan, $\frac{\partial x_{BPM}}{\partial I_{quad}}$, equivalently the uncalibrated

position in the quad. The errorbars are defined as the 95% confidence interval of the slope coefficient.

To calibrate the position in the quad, I use the VRUMER code to determine what initial condition in the quadrupole gives the appropriate BPM response. I first choose an arbitrary starting position $x_{0,q}$, $x'_{0,q}$ and simulate a quad scan. I then apply the Newton-Raphson method to determine the appropriate x_q to give the desired (measured) BPM response, $m_{sim} = m_{data}$ (where $m_{data} = \frac{\partial x_{BPM}}{\partial I_{quad}}$):

$$x_q = x_{0,q} - (m_{sim} - m_{data}) \left(\frac{dm_{sim}}{dx_q} \right)^{-1} \quad (4.3)$$

This allows us to define a calibration factor between the BPM response and the position at the center of each quadrupole,

$$x_q = C_{q,BPM} \times \frac{\partial x_{BPM}}{\partial I_{quad}} \quad (4.4)$$

While this factor will not change for a static version of VRUMER, the `kiersten_quad_scan_v2.m` procedure is set up to do the Newton-Raphson calculation for every set of quad scan data. This was mainly a matter of convenience at the time, as having a lookup table for the calibration factors would result in slight decrease in run time and a loss of flexibility (changes to ring operation would require recalculation of the look-up table, etc). Running VRUMER takes ~ 0.06 seconds, so even for the an entire quad scan (9 points) repeated twice for the Newton-Raphson calculation VRUMER costs ~ 1 second per quad.

This is a description of the horizontal steering method I used to steer the 6

mA beam on November, 2015. The final solution was saved as settings file `kiersten_6mA_151116.csv`.

The procedure for horizontal steering attempts to steer the beam as close as possible to the center of the quads in the first turn, and use two dipoles at the end of the ring to close the orbit. I generated this solution using an existing solution with many turns, but it should be possible to apply this method to a ring with "no-steering" (significant current loss in the first few turns). The procedure is as follows:

1. Set last 2 injection dipoles by scanning currents and identifying smallest rms deviation in first two RQ's after injection. Time: 1 hour.
2. Steer through RQ3 (first turn) by setting current in D1; Repeat injection scan if change was significant. Time: 10 minutes + 1 hour if repeating injection scan.
3. Steer through quads in first turn, setting dipoles D2-34 in order and using quad-as-BPM method to measure position in quads. Time: 2 1/2 hours ($\times 2$ for best results).
4. Close orbit by scanning D34 and D35 currents. Time: 30 minutes
5. Verify orbit quality by running quad scan for 1st turn quad-as-BPM data, and look at multi-turn BPM data to estimate orbit excursions from closed orbit. Time: 30 minutes.

Total (minimum) time for steering: ≈ 6 hours. Time estimates are for total

measurement/ beam-on time, more time should be added for trouble-shooting and general unruly behavior.

4.6.1 *Closing the orbit*

The final step is to set the current in the dipoles near the end of the ring so that the closed orbit is close to the p1 closed orbit. Two dipoles are required for control of x and x' . Naively, one would vary the last two dipoles, D35 and PD-Rec. Unfortunately PD-Rec has significant coupling with the first turn beam position. For a scan of PD-Rec from $8.25 \rightarrow 13.75$ A, the position of the beam in the first BPM varies in the range $\Delta x = \pm 2\text{mm}$. Changing PD-Rec would mean changing all ring dipole settings to compensate, which is undesirable.

It is possible but difficult to optimize the value of PD-Rec. Instead, I assume that the present setting (PD-Rec $I = 11$ A) is reasonably close to the ideal value such that closing the orbit with D34 and D35 will result in a bump in the closed orbit in that neighborhood. It may be possible to infer, based on the difference in the D34 currents optimized for a) steering through RQ69 and RQ70 and b) a closed orbit solution, the size of the orbit bump.

To set D34 and D35, I scan the currents in each and record the BPM response for the first four turns in the first 3 BPMs. I try to minimize the RMS change in position between turn 1 and turn $N \leq 4$ in the first three BPM's. For each BPM 1-3, I define an RMS quantity $\sqrt{\frac{1}{3} [(x_2 - x_1)^2 + (x_3 - x_1)^2 + (x_4 - x_1)^2]}$. In order to find a good closed orbit, I ran 3 scans, increasing the resolution and/or re-centering the scan range for each successive scan. Scan takes ~ 13 minutes to read 3 BPMs

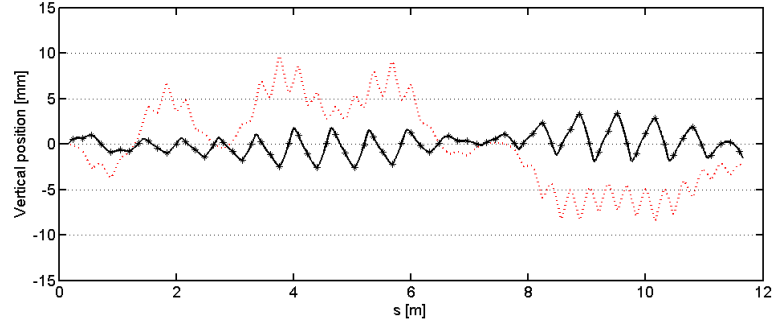
for 11 current settings in each dipole.

4.7 Increasing Vertical Steering Capability

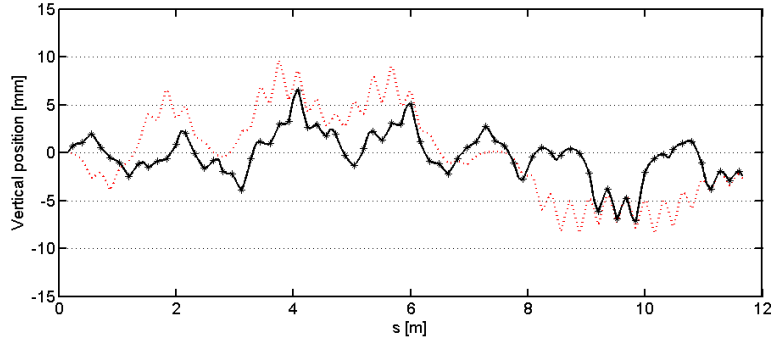
4.8 Comments on steering the Alternative Lattice

Tab. 4.3: Vertical steering algorithms and their performance (RMS position in quads)
for initial condition $y = 0$ mm, $y' = 0$. Subscript indicates quad # counting
downstream from vertical steerer (y_1 is position in first quad downstream from
each RSV).

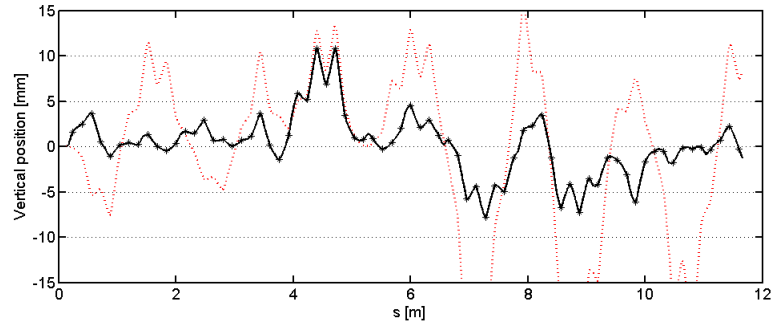
shorthand	Minimization Function	RMS(y_Q) [mm]	RMS(y_Q) [mm] SV limit	RMS(y_Q) [mm] $\sigma = 1$ mm
SV=0	none	4.6	4.6	10.4
y_1	$\ y_1\ $	37.0		
y_3	$\ y_3\ $	1.5	2.2	3.8
y_4	$\ y_4\ $	1.7	2.5	3.4
y_1, y_2	$\sqrt{\frac{1}{2}(y_1^2 + y_2^2)}$	25.9		
y_2, y_3	$\sqrt{\frac{1}{2}(y_1^2 + y_3^2)}$	1.2	2.5	4.2
y_3, y_4	$\sqrt{\frac{1}{2}(y_3^2 + y_4^2)}$	0.98	2.4	3.7
y_1, y_3 (focusing)	$\sqrt{\frac{1}{2}(y_1^2 + y_3^2)}$	1.1	2.5	
y_2, y_4 (defocusing)	$\sqrt{\frac{1}{2}(y_2^2 + y_4^2)}$	0.93	2.6	4.6
y_1, y'_1	$\sqrt{\frac{1}{2}(y_1^2 + (y_2 - y_1)^2)}$	18.7		
y_2, y'_2	$\sqrt{\frac{1}{2}(y_2^2 + (y_3 - y_2)^2)}$	1.1	2.2	
y_3, y'_3	$\sqrt{\frac{1}{2}(y_2^2 + (y_4 - y_3)^2)}$	1.3	2.2	
y_1, y_2, y_3, y_4	$\sqrt{\frac{1}{4}(y_1^2 + y_2^2 + y_3^2 + y_4^2)}$	0.95	2.4	5.0



(a) Vertical steering for perfect alignment, no SV limit. Steering by minimizing $\|y_4\|$. Red dotted trace is vertical solution without steering corrections.



(b) Vertical steering for perfect alignment, SV current limited to 2 A.



(c) Vertical steering for misalignment of $\sigma = 1$ mm, SV current limited to 2 A.

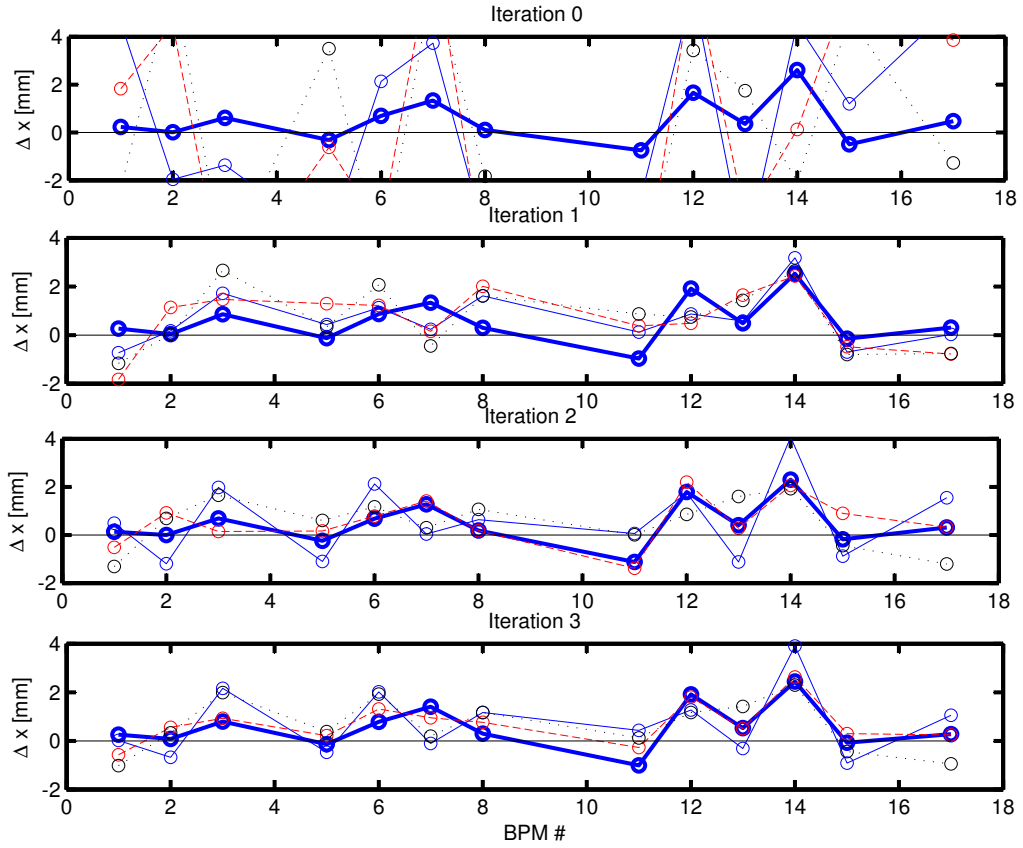


Fig. 4.7: BPM response for first 4 turns, for D34, D35 currents listed in table ??.

1st turn: heavy blue trace. 2nd turn: solid blue. 3rd turn: long dash red. 4th turn: short dash black.

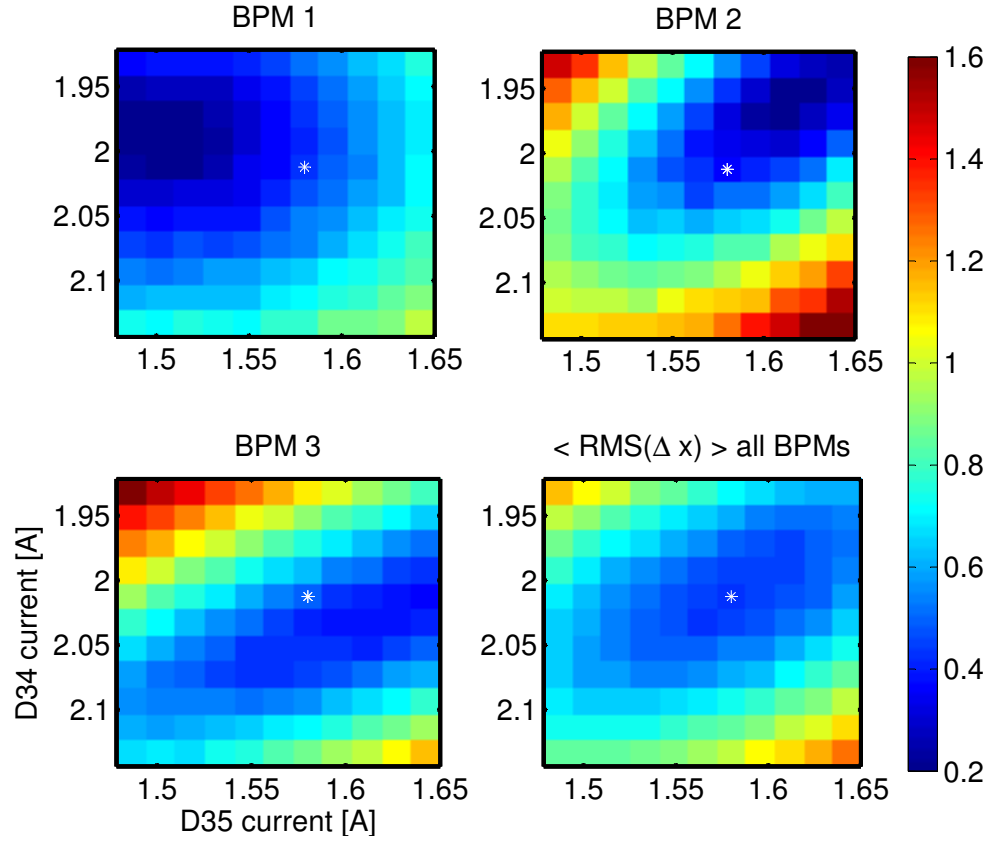


Fig. 4.8: Scan results for first 3 BPMs for iteration 3 in table ?? . Color scale is rms value of Δx over first 4 turns [mm], white asterisk indicates optimal setting (D34=2.0129 A, D35=1.5802 A)